Inorg. Chem. **2004**, *43*, 8110–8118

Electronic Structure of Bent Titanocene Complexes with Chelated Dithiolate Ligands

J. Jon A. Cooney, Matthew A. Cranswick, Nadine E. Gruhn, Hemant K. Joshi, and John H. Enemark*

Department of Chemistry, The University of Arizona, Tucson, Arizona 85721

Received June 17, 2004

Gas-phase photoelectron spectroscopy and density functional theory have been utilized to investigate the interactions between the p orbitals of dithiolate ligands and d orbitals of titanium in bent titanocene complexes as minimum molecular models of active site features of pyranopterin Mo/W enzymes. The compounds $Cp_2Ti(S–S)$ [where (S–S) is 1,2-ethenedithiolate ($S_2C_2H_2$), **1**, 1,2-benzenedithiolate (bdt), **2**, or 1,3-propanedithiolate (pdt), **3**, and Cp^- is cyclopentadienyl] provide access to a formal 16-electron d^0 electronic configuration at the metal. A "dithiolate-folding-effect" involving an interaction of metal and sulfur orbitals is demonstrated in complexes with arene- and enedithiolates. This effect is not observed for the alkanedithiolate in complex **3**.

Introduction

Coordination by the sulfur atoms of one or two ene-1,2-dithiolate (dithiolene) ligands of the novel substituted pyranopterindithiolate ("molybdopterin"[1]) is a common structural feature of mononuclear molybdenum-containing enzymes.[2−5] These enzymes catalyze a wide range of oxidation/reduction reactions in carbon, sulfur, and nitrogen metabolism. Figure 1 shows the structure of the active site of sulfite oxidase, a representative example[6,7] of the coordination of the pyranopterindithiolate.

The exact role of the pyranopterindithiolate coordination in the overall catalytic cycle of molybdenum enzymes is not yet established.[8] The unusual ability of ene-1,2-dithiolate ligands to stabilize metals in multiple oxidation states has long been recognized.[9] Proposed roles for the pyranopterindithiolate ligand include functioning as an electron-transfer conduit from the metal to other prosthetic groups[10] and as a modulator of the oxidation/reduction potential of the metal site.[10]

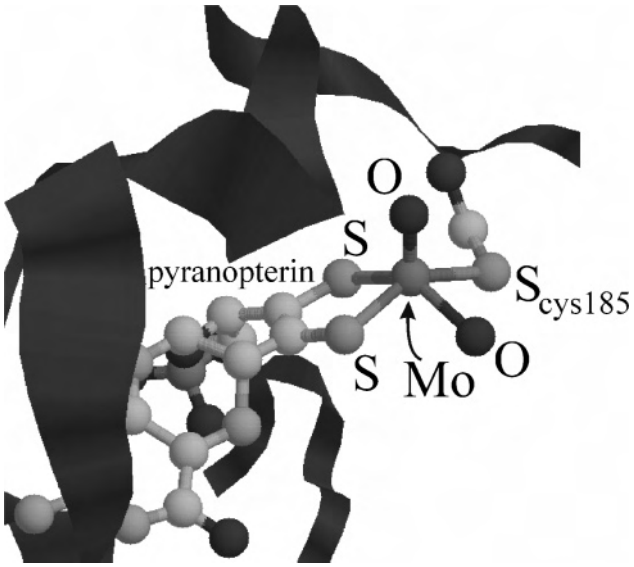

Figure 1. Active site of chicken liver sulfite oxidase illustrating a pyranopterin dithiolate coordinated to the Mo center.

The known bent-metallocenedithiolate class of compounds (Cp_2M(dithiolate), M = Ti, Zr, Hf, V, Nb, Mo, and W and

* Author to whom correspondence should be addressed. E-mail: jenemark@u.arizona.edu.

(1) Rajagopalan, K.; Johnson, J. L. *J. Biol. Chem.* **1992**, *267* (15), 10199−10202.
(2) Hille, R. *Chem. Rev.* **1996**, *96*, 2757−2816.
(3) Sigel, A.; Sigel, H. *Molybdenum and Tungsten: Their Roles in Biological Processes*; Metals Ions in Biological Systems Vol. 39; Dekker: New York, 2002.
(4) Garner, D. C.; Banham, R.; Cooper, S. J.; Davies, E. S.; Stewart, L. J. In *Handbook on Metalloproteins*; Bertini, I., Sigel, A., Sigel, H., Eds.; Marcel Dekker: New York, 2001; pp 1023−1090.
(5) Burgmayer, S. J. N. *Prog. Inorg. Chem.* **2004**, *52*, 491−537.
(6) Kisker, C.; Schindelin, H.; Pacheco, A.; Wehbi, W.; Garrett, R. M.; Rajagopalan, K. V.; Enemark, J. H.; Rees, D. C. *Cell* **1997**, *91*, 973−983.
(7) Kisker, C. *Handbook of Metalloproteins*; Messerschmidt, A., Huber, R., Poulos, T., Weighardt, K., Eds.; John Wiley & Sons Ltd.: New York, 2001; Vol. 2, pp 1121−1135.
(8) Schindelin, H.; Kisker, C.; Rees, D. *J. Biol. Inorg. Chem.* **1997**, *2* (6), 773−781.
(9) Eisenberg, R. *Prog. Inorg. Chem.* **1970**, *12*, 295−369.
(10) Inscore, F. E.; McNaughton, R.; Westcott, B.; Helton, M. E.; Jones, R.; Dhawan, I. K.; Enemark, J. H.; Kirk, M. L. *Inorg. Chem.* **1999**, *38*, 1401−1410.

10.1021/ic049207+ CCC: $27.50
Published on Web 11/13/2004

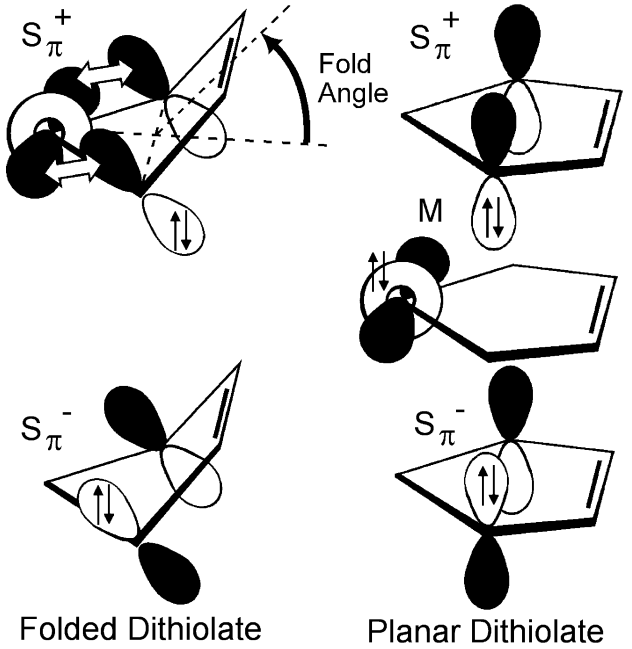

Figure 2. Representations of the valence orbitals of folded versus flat dithiolates. In the d^0 case the metal orbital (M) is empty and the S_π^+ orbital can interact, with folding. In the d^2 case the metal orbital (M) is filled and a planar orientation minimizes a filled−filled interaction. The S_π^- orbital does not have the right symmetry to interact with the metal orbital.

Cp = η^5-cyclopentadienyl) provides access to a range of small molecules which contain the dithiolate ligation.[11] These molecules are useful as models of the pyranopterindithiolate system of the mononuclear molybdenum-containing enzymes. There are molecules within the class that contain d^0, d^1, and d^2 electron configurations, the same electron configurations as the metal-center during the enzyme catalytic cycle. The M−S−C−C−S metallocycle of metallocenedithiolates can show folding along the S−S vector, as illustrated in Figure 2.[12] The range of fold angles of metallocenedithiolates encompass the range of fold angles observed in protein crystal structures (7−30°).[6,12−16] Molecules of this class are known with a variety of different dithiolate ligands, many of which have been crystallographically characterized.[11] Furthermore, many of these molecules are amenable to gas-phase photoelectron spectroscopy (PES), permitting the study of their electronic structure.

A general bonding description of Cp_2MX_2 compounds is well understood,[17−19] and Lauher and Hoffmann first explained the variation in fold angle for Cp_2M(dithiolate) compounds as due to the occupancy of the metal d-orbital in the equatorial plane (M_{ip}) with respect to the dithiolate ligand. This orbital is empty for the folded d^0 molecules and filled for the more nearly planar d^2 molecules. The observed folding for the d^0 systems facilitates interaction of the filled S_π orbitals with the empty M_{ip} orbital, as shown in Figure 2. In contrast, for the d^2 metal system, folding the ligand would bring a filled S_π orbital into close proximity with the filled M_{ip} orbital. Hence, the M−S−C−C−S metallocycle being planar minimizes the filled−filled interaction between the ligand and metal-based obitals.

Recent theoretical studies have supported this theory; Reinhold et al.[20] extended the work of Lauher and Hoffmann[17] with theoretical studies on binuclear titanocene-based systems and molecules with oxygen in place of sulfur as the ligating atom. The paper concluded that the dithiolene folding stabilizes the molecule and lowers the total energy of the system. However, folding also destabilizes a Ti−Cp bonding orbital, which raises the total energy of the system. Thus, there is a mutual ligand influence between the dithiolate and the cyclopentadienyl ligands. The degree of folding is a balance between the competing donor abilities of the folded chelate ligand and the coordinating Cp^- rings.

Experimental evidence supporting the Lauher and Hoffmann[17] description of the electronic structure includes our recent PES study of flat Cp_2Mo(bdt) and folded Cp_2Ti(bdt). The gas-phase photoelectron spectra of Cp_2M(bdt) (M = Ti and Mo) clearly show that under favorable conditions the ionizations from primarily metal-based orbitals and primarily S_π-based orbitals can be experimentally distinguished from one another.[16,21] The S_π-based orbitals form a symmetric and antisymmetric pair. The symmetric (S_π^+) orbital has the right symmetry and energy to match the metal in-plane orbital upon folding of the dithiolate unit, whereas the antisymmetric sulfur (S_π^-) orbital does not (Figure 2). The substantial mixing of the out-of-plane S_π^+ orbital and metal in-plane orbital upon folding is shown experimentally in the PE spectra of Cp_2Ti(bdt) by the increase in intensity of the S_π^+ band relative to the S_π^- band with change in ionization source from He I to He II. From previous experimental studies[22−24] and calculations of atomic photoionization cross-sections,[25] it is expected that ionizations from molecular orbitals with significant Ti 3d contributions will increase in intensity compared to ionizations of primarily S 3p character when data collected with a He II photon source is compared to data collected with a He I photon source. Thus, in the case of Cp_2Ti(bdt), which has formally a Ti(IV) d^0 metal center, the dithiolate ligand can be thought of as a six-electron donor. Each of the thiolate σ-orbitals provides two electrons, and two additional electrons come from the S_π^+ orbital. Thus,

(11) Fourmigué, M. *Coord. Chem. Rev.* **1998**, *178−180* (1), 823−864.
(12) The fold angle is the acute angle between the vector from the metal to the centroid of the two sulfur atoms and the vector from this centroid to that of the two carbon atoms of the metallacycle (Figure 2).
(13) Rebelo, J.; Dias, J.; Huber, R.; Moura, J.; Romão, M. *J. Biol. Inorg. Chem.* **2001**, *6* (8), 791−800.
(14) Enroth, C.; Eger, B. T.; Okamoto, K.; Nishino, T.; Nishino, T.; Pai, E. F. *Proc. Natl. Acad. Sci. U.S.A.* **2000**, *97* (20), 10723−10728.
(15) Li, H. K.; Temple, C.; Rajagopalan, K.; Schindelin, H. *J. Am. Chem. Soc.* **2000**, *122* (32), 7673−7680.
(16) Joshi, H. K.; Cooney, J. J. A.; Inscore, F. E.; Gruhn, N. E.; Lichtenberger, D. L.; Enemark, J. H. *Proc. Natl. Acad. Sci. U.S.A.* **2003**, *100* (7), 3719−3724.
(17) Lauher, J. W.; Hoffmann, R. *J. Am. Chem. Soc.* **1976**, *98* (7), 1729−1742.
(18) Green, J. C. *Struct. Bonding (Berlin)* **1981**, *43*, 37−112.
(19) Green, J. C. *Chem. Soc. Rev.* **1998**, *27* (4), 263−272.
(20) Flemmig, B.; Strauch, P.; Reinhold, J. *Organometallics* **2003**, *22*, 1196−1202.
(21) Joshi, H. K. Ph.D. Dissertation, University of Arizona, Tucson, AZ, 2003.
(22) Glass, R. S.; Gruhn, N. E.; Lichtenberger, D. L.; Lorance, E.; Pollard, J. R.; Birringer, M.; Block, E.; DeOrazio, R.; He, C.; Shan, Z.; Zhang, X. *J. Am. Chem. Soc.* **2000**, *122* (21), 5065−5074.
(23) Green, J. C. *Acc. Chem. Res.* **1994**, *27* (5), 131−137.
(24) Gelius, U. *J. Electron Spectrosc. Relat. Phenom.* **1974**, *5*, 985−1057.
(25) Yeh, J.; Lindau, I. *At. Data Nucl. Data Tables* **1985**, *32* (1), 1−155.

folding the dithiolate ligand effectively stabilizes $Cp_2Ti(bdt)$ as an 18-electron complex.

Structural studies of molybdenum complexes of the type (Tp*)MoE(dithiolate) [where E is O or NO, Tp* is hydrotris-(3,5-dimethyl-1-pyrazolyl)borate, and the dithiolates are 1,2-benzenedithiolate, 3,6-dichloro-1,2-benzenedithiolate, and 2,3-quinoxalinedithiolate] also showed that the fold angle of the dithiolate metallacycle along the S−S vector (Figure 2) varies in a way that is dependent upon the occupation of a d orbital that is in the equatorial plane.[26,27] Previous studies of $\{MoOS_4\}$ systems with monodentate and bidentate thiolate ligands using MCD, electronic absorption, and EPR spectroscopy and theoretical calculations demonstrated that the amount of orbital interaction between the sulfur ligands and the metal showed a strong dependence on the orientation of the S 3p lone pair orbitals.[28,29] The molecular orbital calculations predicted that for $\{MoOS_4\}$ complexes with chelating ligands the energies of the singly occupied in-plane metal orbital and the filled S p_π orbitals are similar—for $[MoO(SMe)_4]^-$ the energy difference between the metal orbital and the highest occupied S p_π orbitals varies from 0.4 to 1.3 eV depending on the orientation of the S 3p lone pair orbitals.[28] Subsequent anion photoelectron spectroscopy work on the $\{MoOS_4\}$ systems further confirmed that the relative energy levels of the metal- and sulfur-based orbitals were strongly influenced by the orientation of the S 3p lone pair orbitals.[30] The anion PES results also clearly show that the singly occupied in-plane Mo d orbital and filled S p_π orbitals have similar energies—the vertical detachment energies of the Mo d orbitals and first S p_π orbitals are 3.46 and 4.25 eV for $[MoO(SPh)_4]^-$, 3.89 and 4.69 eV for $[MoO(p\text{-}SPhCl)_4]^-$, 3.70 and 4.12 eV for $[MoO(bdt)_2]^-$, and 4.15 and 4.61 eV for [MoO(3,6-dichloro-1,2-benzenedithiolate)$_2$]$^-$, respectively.[30]

The goal of this study is to investigate possible roles of the −C═C− linkage between the sulfur atoms in the pyranopterindithiolate unit by comparing the electronic structures of relatively simple complexes with saturated and unsaturated dithiolate chelate skeletons. The Cp_2Ti(dithiolate) complexes are well suited for these comparative studies because the compounds are readily accessible and sufficiently volatile for gas-phase PES studies. The basic structures of these bent metallocenes are well-known, and we have previously investigated the electronic structure of $Cp_2Ti(bdt)$ in detail.[16] Here we use gas-phase PES, absorption spectroscopy, and theoretical calculations to compare the properties of the analogous complexes of the minimal unsaturated dithiolate ligand system 1,2-ethenedithiolate with those of the saturated ligand 1,3-propanedithiolate. The 1,2-ethenedithiolate offers dithiolene ligation without the interaction of the benzene ring apparent in 1,2-benzenedithiolate. The dithiolate ligand and metal of bis(cyclopentadienyl)titanium 1,3-propanedithiolate (**3**) form a saturated six-membered metallocycle. This complex has not been crystallographically characterized, but it is presumably similar to that of bis-(cyclopentadienyl)vanadium 1,3-propanedithiolate,[31] as supported here by DFT geometry optimization calculations. The metallocycle in **3** could form either a chair or boat conformation, with a fold along the S−S vector as shown in Figure 3; cf. the vanadium analogue which takes up the chair conformation.[31] Thus, this molecule (**3**) would have a overall conformation similar to that of the dithiolene compounds (**1** and **2**) but without −C═C− linkage to electronically couple the pπ orbitals on the two S atoms.

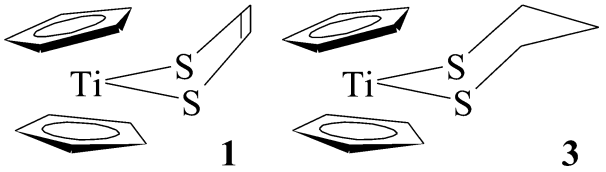

Figure 3. Representations of bis(cyclopentadienyl)titanium 1,2-ethenedithiolate (**1**) and bis(cyclopentadienyl)titanium 1,3-propanedithiolate (**3**).

Experimental Methods

General Methods. Electronic absorption (dichloromethane solutions on a modified Cary 14 with OLIS interface, 280−900 nm) and infrared (KBr disks on a Nicolet Avatar ESP 360 FT-IR, 4000−400 cm^{-1}) spectroscopies and mass spectrometry (direct ionization on a JEOL HX110) were used to identify the compounds. The compounds Cp_2Ti(ethenedithiolate), **1**, Cp_2Ti(1,2-benzenedithiolate), **2**,[32,33] and Cp_2Ti(1,3-propanedithiolate), **3**,[34] were synthesized according to published procedures and under anaerobic conditions using either an inert-atmosphere glovebag, drybox, or standard Schlenk line techniques.

Photoelectron Spectroscopy. Photoelectron spectra were recorded using an instrument, procedures, and calibration that have been described in more detail.[35] During data collection the instrument resolution (measured using fwhm of the argon $^2P_{3/2}$ peak) was 0.020−0.030 eV. The sublimation temperatures were (°C, 10^{-4} Torr, monitored using a "K" type thermocouple passed through a vacuum feed-through and attached directly to the sample cell) 195−205 for compound **1**, 190−200 for compound **2**, and 195−210 for compound **3**.

In Figure 4 the vertical length of each data mark represents the experimental variance of that point. The valence ionization bands are represented analytically with the best fit of asymmetric Gaussian peaks.[36] The number of peaks used in a fit was based solely on the features of a given band profile. The peak positions are reproducible to about ±0.02 eV (≈3σ). The parameters describing an individual Gaussian peak are less certain when two or more peaks are close in energy and overlap.

(26) Joshi, H. K.; Inscore, F. E.; Schirlin, J. T.; Dhawan, I. K.; Carducci, M. D.; Bill, T. G.; Enemark, J. H. *Inorg. Chim. Acta* **2002**, *337*, 275−286.
(27) Inscore, F. E.; Joshi, H. K.; McElhaney, A. E.; Enemark, J. H. *Inorg. Chim. Acta* **2002**, *331*, 246−256.
(28) McMaster, J.; Carducci, M. D.; Yang, Y.-S.; Solomon, E. I.; Enemark, J. H. *Inorg. Chem.* **2001**, *40*, 687−702.
(29) McNaughton, R. L.; Tipton, A. A.; Rubie, N. D.; Conry, R. R.; Kirk, M. L. *Inorg. Chem.* **2000**, *39*, 5697−5706.
(30) Wang, X.-B.; Inscore, F. E.; Yang, X.; Cooney, J. J. A.; Enemark, J. H.; Wang, L.-S. *J. Am. Chem. Soc.* **2002**, *124*, 10182−10191.
(31) Stephan, D. W. *Inorg. Chem.* **1992**, *31*, 4218−4223.
(32) Klapötke, T.; Köpf, H. *Z. Anorg. Allg. Chem.* **1988**, *558*, 217−222.
(33) Lowe, N. D.; Garner, C. D. *J. Chem. Soc., Dalton Trans.* **1993**, 2197−2207.
(34) Shaver, A.; McCall, J. M. *Organometallics* **1984**, *3* (12), 1823−1829.
(35) Westcott, B. L.; Gruhn, N. E.; Enemark, J. H. *J. Am. Chem. Soc.* **1998**, *120*, 3382−3386.
(36) Lichtenberger, D. L.; Copenhaver, A. S. *J. Electron Spectrosc. Relat. Phenom.* **1990**, *50* (2), 335−352.

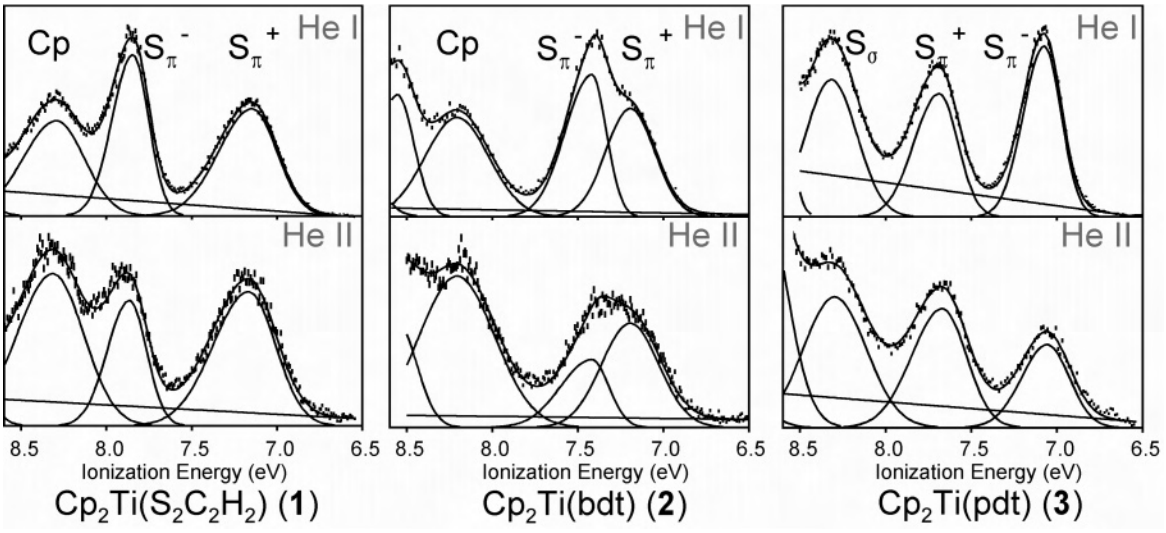

Figure 4. Photoelectron spectra of the low-energy valence region of **1**−**3**.

Theoretical Methods. The Amsterdam density functional theory suite (ADF 2003.01, using the standard parameters except for the options given in parentheses) was used to study the electronic structures of the compounds **1**−**3**.[37−41] The optimized geometries of **1**−**3** (Tables S1−S3, Supporting Information) were obtained in C_s symmetry. The geometries of the molecules were constructed such that the C_s plane, which bisects the metal atom and all 3 ligands, was coincident with the *xz* plane, and such that the Cp rings were staggered with respect to each other. A generalized gradient approximation, with the exchange correction of Becke[42] and the correlation correction of Lee et al. (GGA BLYP),[43] was used for calculations of the optimized geometries. Further asymptotically correct time-dependent DFT calculations (model SAOP)[44] using the optimized geometric coordinates were carried out for predictions of the electronic absorption spectra (excitation).[45] The calculations employed triple-ζ basis sets with Slater type orbitals and polarization functions for all elements (TZ2P). Calculations on the ground-state molecules were performed in the spin-restricted mode (restricted). ΔSCF calculations of the ionized states were performed at the fixed geometry of the neutral molecule, with one electron removed from the relevant orbital. The ΔSCF estimate of the ionization energy is the difference between the calculated total energy of the ionized state and that of neutral ground-state molecule. A linear correction was applied for comparison of the calculated and the observed energies; i.e., calculated ΔSCF energies and calculated orbital energy estimates of the ionization energies were shifted by the difference between the observed first ionization energy and the negative of the calculated eigenvalue of the HOMO. Estimates of transition energies were made using both time-dependent density functional theory and the Slater transition state formalism in which the energy of an electronic transition is determined by the orbital-energy difference from a stationary-point calculation where the population of the ground-state molecular orbital (MO) is lowered by 0.5 and the population of the excited-state MO is increased by 0.5 (occupations).[46] Spin-unrestricted calculations (unrestricted) were performed on the relevant excited states at the fixed geometry of the neutral molecule. For these spin-unrestricted calculations the occupancy of the MO's were chosen to have overall α-spin, i.e., chosen to represent singlet−singlet transitions.

Results and Discussion

Photoelectron Spectroscopy. The low-energy valence regions of the gas-phase photoelectron spectra of **1**−**3** collected with both He I and He II photon sources are presented in Figure 4.

The first, second, and third bands of the photoelectron spectra of the Cp_2Ti(1,2-ethenedithiolate) molecule (**1**) occur at 7.15, 7.85, and 8.29 eV, respectively. The ratio of areas of these bands changes with change of ionization source from He I (1st:2nd:3rd = 1.00:0.94:0.94) to He II (1.00:0.59:1.21). Thus, upon a change from He I to He II ionization source, the second band decreases in intensity and the third band increases in intensity, relative to the intensity of the first band.

The photoelectron spectra of **2**, as reported earlier,[16] show two overlapping ionization bands at 7.20 and 7.42 eV with the next band at 8.21 eV. The ratio of the areas of these three peaks changes as the ionization source changes from He I (1st:2nd:3rd = 1.00:1.10:1.20) to He II (1.00:0.55:1.90). However, areas of the first and second bands are less certain because the ionizations are close in energy. Again, the second band decreases in intensity, and the third band increases in intensity, relative to the intensity of the first band with change from He I to He II ionization source.

The behavior of the bands in **1** and **2** is similar. The valence orbitals of these titanocene-based dithiolate complexes must all contain significant ligand character, given that the titanium center is formally d^0. According to the scheme devised by Lauher and Hoffmann[17] the HOMO and

(37) Baerends, E. J.; Ellis, D. E.; Ros, P. *Chem. Phys.* **1973**, *2*, 41−51.
(38) Fonseca Guerra, C.; Snijders, J. G.; te Velde, G.; Baerends, E. J. *Theor. Chem. Acc.* **1998**, *99*, 391−399.
(39) te Velde, G.; Bickelhaupt, F. M.; Baerends, E. J.; Fonseca Guerra, C.; Van Gisbergen, S. J. A.; Snijders, J. G.; Ziegler, T. *J. Comput. Chem.* **2001**, *22* (9), 931−967.
(40) te Velde, G.; Baerends, E. J. *J Comput. Phys.* **1992**, *99* (1), 84−98.
(41) Versluis, L.; Ziegler, T. *J. Chem. Phys.* **1988**, *88*, 322−329.
(42) Becke, A. D. *Phys. Rev. A* **1988**, *38*, 3098−3100.
(43) Lee, C.; Yang, W.; Parr, R. G. *Phys. Rev. B* **1988**, *37*, 785−789.
(44) Schipper, P. R. T.; Gritsenko, O. V.; Van Gisbergen, S. J. A.; Baerends, E. J. *J. Chem. Phys.* **2000**, *112* (3), 1344−1352.
(45) Van Gisbergen, S. J. A.; Snijders, J. G.; Baerends, E. J. *Comput. Phys. Commun.* **1999**, *118*, 119−138.
(46) Slater, J. C. *Adv. Quantum Chem.* **1972**, *6*, 1−92.

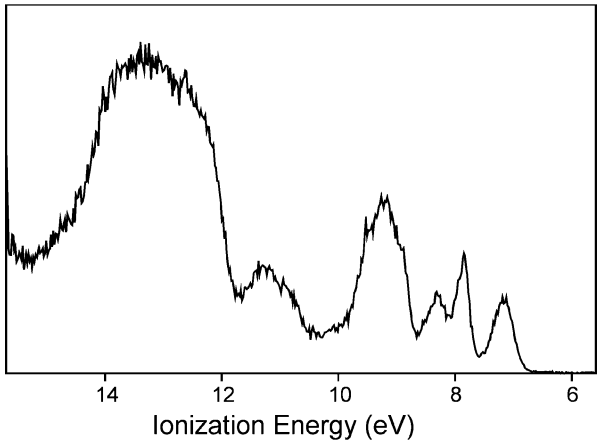

Figure 5. Extended He I photoelectron spectrum of **1**.

HOMO − 1 are S_π-based. The symmetric (S_π^+) orbital has the proper symmetry to interact with the empty metal orbital upon folding. The intensity increase with He II ionization that is evident in the first band relative to the second is consistent with the lowest energy peak containing some contributions from Ti, and hence, it is assigned as S_π^+. The second band is assigned to the S_π^- ionization which does not mix significantly with the empty Ti d acceptor orbital. This analysis compares well with that of $(\eta^5\text{-}^t\text{BuC}_5\text{H}_4)_2\text{Zr}(\text{Se}_2\text{C}_6\text{H}_4)$,[47] although for this molecule the first band was assigned as a combination of Se_π^+ and Se_π^- ionizations that are not greatly split in energy.

For both **1** and **2**, the two peaks at lower energy decrease in intensity with respect to the third, higher energy band near 8.2 eV, consistent with the third band being carbon-based. This assignment of the third ionization is consistent with a Ti−Cp bonding orbital being destabilized, as proposed by Reinhold et al.[20] The spectra of **1** can be compared with those of Cp_2TiCl_2. The lowest energy ionizations of Cp_2TiCl_2 are located from about 8.5−10 eV and are assigned to Cp ionizations.[48] The corresponding bands of **1** include the band at 8.29 and are among the bands between 8.9 and 9.8 eV (See Figure 5). However, for Cp_2TiCl_2, the separation between the first and second Cp bands (0.4 eV) is less than the corresponding separation in **1** (0.6 eV). This difference is consistent with the mutual ligand influence destabilizing a Cp-based orbital.

The photoelectron spectra of the $Cp_2Ti(pdt)$ molecule (**3**) again show three distinct ionization bands, at 7.08, 7.69, and 8.32 eV. The ratio of the areas changes with change from He I (1st:2nd:3rd = 1.00:0.84:1.09) to He II (1.00:1.64:2.07) as the ionization source. The area of the first band decreases significantly relative to that of the second band with change in photon source from He I to He II. This behavior contrasts with that of **1** and **2** and is consistent with the second, *higher* energy peak containing contributions from Ti. Therefore, the higher energy peak is assigned to S_π^+.[16,21] The lower energy peak in **3** is assigned to the S_π^- ionization, which again does not mix significantly with the empty Ti d acceptor orbital. This reversal in energy of the S_π^+ and S_π^- occupied orbitals in **3** when compared with **1** and **2** is shown in Figure 6. An additional difference in the spectra shown for **3** is observed for the third ionization, near 8.2 eV. For **1** and **2**, the intensity of this band relative to the two lower energy features increases with He II ionization, as expected for a carbon-based orbital (see above). However, for **3** the third band does not increase in intensity significantly relative to the second band (He I, 2nd:3rd = 1.00:1.30; He II, 2nd:3rd = 1.00:1.26), and it is therefore assigned as primarily sulfur-based.

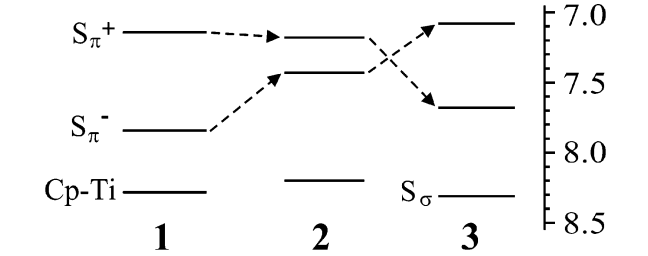

Figure 6. Energy level diagram of the ionization energies of **1**−**3**, determined by PES.

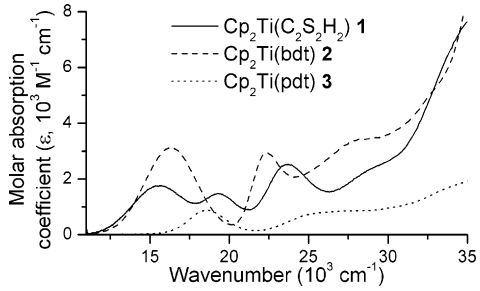

Figure 7. Electronic absorption spectra of **1**−**3**.

Electronic Absorption Spectroscopy. Figure 7 shows the electronic absorption spectra for **1**−**3**. The electronic absorption spectrum of **1** shows peaks at 15 500 (ϵ = 1750), 19 300 (1470), and 23 700 (2520), a shoulder at 29 500 (2520 M^{-1} cm^{-1}), and very intense UV transitions starting at 31 000 cm^{-1}. That of **2** shows peaks at 16 400 (ϵ = 3140) and 22 400 (2930), a shoulder at 28 700 (3430 M^{-1} cm^{-1}), and very intense UV transitions starting at 30 000 cm^{-1}. The spectrum of **3** shows a peak at 18 600 (ϵ = 880), a shoulder at 27 800 (860 M^{-1} cm^{-1}), and intense UV transitions starting at 34 000 cm^{-1}.

Computational Results. The electronic structures of **1**−**3** were calculated using C_s symmetry and geometry-optimized molecular structures. The geometry optimizations are carried out on isolated molecules,[39] corresponding to the conditions of the PES experiment. The calculated molecular structures of **1** and **2** compare well with the reported structures determined from X-ray crystallography.[49,50] As a result of geometry optimization, the dithiolate fold angle differs from the crystallographic fold angle of 46.1 [49] to 44.3° in **1** and from 46.0 [50] to 41.6° in **2** (see Supporting Information). In C_s symmetry there are two isomers of **1** and **2**, using only

(47) Guimon, C.; Pfister-Guillouzo, G.; Meunier, P.; Gautheron, B.; Tainturier, G.; Pouly, S. *J. Organomet. Chem.* **1985**, *284* (3), 299−312.
(48) Cauletti, C.; Clark, J. P.; Green, J. C.; Jackson, S. E.; Fragala, I. L.; Ciliberto, E.; Coleman, A. W. *J. Electron Spectrosc. Relat. Phenom.* **1980**, *18* (1−2), 61−73.
(49) Kutoglu, A. *Acta Crystallogr., Sect. B* **1973**, *29* (12), 2891−2897.
(50) Kutoglu, A. *Z. Anorg. Allg. Chem.* **1972**, *390*, 195−209.

Table 1. Experimental and Calculated Orbital Ionization Energies (eV) for the Ionizations from Valence Orbitals of **1**−**3**[a]

	$Cp_2Ti(S_2C_2H_2)$ (**1**)				$Cp_2Ti(bdt)$ (**2**)				$Cp_2Ti(pdt)$ (**3**)			
method	PES (assgnt)	BLYP orbital energy	SAOP orbital energy	ΔSCF	PES (assgnt)	BLYP orbital energy	SAOP orbital energy	ΔSCF	PES (assgnt)	BLYP orbital energy	SAOP orbital energy	ΔSCF
1st ionizatn	7.15 (S_π^+)	−4.43 (7.15)	−8.42 (7.15)	6.80 (7.15)	7.20 (S_π^+)	−4.59 (7.20)	−8.62 (7.20)	6.74 (7.20)	7.08 (S_π^-)	−4.30 (7.08)	−8.33 (7.08)	6.77 (7.08)
2nd ionizatn	7.85 (S_π^-)	−5.12 (7.84)	−9.14 (7.87)	7.52 (7.87)	7.42 (S_π^-)	−4.75 (7.36)	−8.81 (7.39)	6.95 (7.41)	7.69 (S_π^+)	−4.90 (7.68)	−8.91 (7.66)	7.18 (7.49)
3rd ionizatn	8.29 (Cp^-)	−5.58 (8.30)	−9.63 (8.36)	7.85 (8.20)	8.21 (Cp^-)	−5.60 (8.21)	−9.69 (8.27)	7.70 (8.11)	8.32 (S_σ)	−5.44 (8.22)	−9.46 (8.21)	7.84 (8.15)

[a] PES: experimental vertical ionization energy. BLYP and SAOP orbital energy: the calculated orbital eigenvalue. Values in parentheses are the orbital and ΔSCF energies shifted so that the highest occupied orbital energy correlates with the experimental first ionization energy.

Cp rings that are staggered with respect to each other. However, the isomers differ only by a rotation of the two Cp ligand rings—a change which has been shown to be low in energy.[51] The crystal structure of **3** has not been elucidated but should be similar to that of bis(cyclopentadienyl)-vanadium 1,3-propanedithiolate.[31] There are four possible C_s symmetric isomers of **3**, two in boat and two in chair conformations (using only Cp rings that are staggered with respect to each other). The lowest energy (chair) isomer was used for the interpretations of the spectral data, as the higher energy isomers were very similar (see Supporting Information). The two boat isomers of **3** only differ by a rotation of the Cp^- ligands; likewise the two chair isomers. The dithiolate fold angle of **3** from geometry optimization (48.6°) compares well with the crystallographic fold angle of 43.6° in bis(cyclopentadienyl)vanadium 1,3-propanedithiolate.[31]

For **1**, the calculated C−C bond lengths of the Cp ring range from 1.418 to 1.431 Å, average 1.423 Å, the distances of the centroid of these rings to the metal atom are 2.153 and 2.132 Å, and in the M−S−C−C−S metallocycle the M−S bond lengths are 2.468 Å, the S−C bond lengths are 1.747 Å, the C−C bond length is 1.370 Å, and the S−M−S angle is 83.3°. The C−C bond lengths of the Cp ring of the crystal structure[49] of **1** range from 1.386 to 1.412 Å, average 1.400 Å, and the distances of the centroid of these rings to the metal atom are 2.081 and 2.057 Å, and in the M−S−C−C−S metallocycle the M−S bond lengths are 2.404 and 2.430 Å, the S−C bond lengths are 1.737 and 1.741 Å, the C−C bond lengths are 1.342 Å, and the S−M−S angle is 83.2°.

For **2**, the calculated C−C bond lengths of the Cp ring range from 1.417 to 1.433 Å, average 1.424 Å, the distances of the centroid of these rings to the metal atom are 2.161 and 2.134 Å, and in the M−S−C−C−S metallocycle the M−S bond lengths are 2.449 Å, the S−C bondlengths are 1.773 Å, the C−C bond length is 1.430 Å, and the S−M−S angle is 82.6°. The C−C bond lengths of the Cp rings of the two molecules in the crystal structure[50] of **2** range from 1.316 to 1.442 Å, average 1.382 Å, the distances of the centroids of these rings to the metal atoms are 2.040, 2.073, 2.053, and 2.075 Å, and in the M−S−C−C−S metallocycles the M−S bond lengths are 2.411, 2.418, 2.405, and 2.423 Å, the S−C bond lengths are 1.764, 1.736, 1.754, and 1.738 Å, the C−C bondlengths are 1.410 and 1.412 Å, and the S−M−S angles are 81.9 and 82.2°.

For **3**, the calculated C−C bond lengths of the Cp ring range from 1.415 to 1.436 Å, average 1.424 Å, the distances of the centroid of these rings to the metal atom are 2.154 and 2.192 Å, and in the M−S−C−C−C−S metallocycle the M−S bond lengths are 2.420 Å, the S−C bond lengths are 1.864 Å, the C−C bond lengths are 1.543 Å, and the S−M−S angle is 91.8°. Those of the crystal structure of bis(cyclopentadienyl)vanadium 1,3-propanedithiolate[31] range from 1.357 to 1.406 Å, average 1.386 Å, the distances of the centroid of these rings to the metal atom are 1.976 and 1.986 Å, and in the M−S−C−C−C−S metallocycle the M−S bond lengths are 2.424 and 2.430 Å, the S−C bond lengths are 1.811 and 1.818 Å, the C−C bond lengths are 1.511 and 1.517 Å, and the S−M−S angle is 86.9°.

The C−S bond length of **3** is ∼0.1 Å longer than those in **1** and **2**, consistent with the ene group coupling the sulfur atoms in **1** and **2**. This difference is comparable with that seen for $Cp_2Mo(dmit)$ upon oxidation to form $[Cp_2Mo(dmit)][AsF_6]$,[52] where the bond length differences in the ligand are assigned to the ligand adopting a more dithioketonic character with increase in oxidation state.

DFT calculations provide additional insight into the metal−dithiolate interactions and indicate that upon dithiolate folding the mixing of metal d and sulfur p_π orbitals can be favored by their energy and symmetry match. The energies of the ionizations observed for molecules **1**−**3** by photoelectron spectroscopy match those calculated by the ΔSCF method and by comparison of orbital energies (Table 1).

Contour plots of the orbitals for **1** and **3** that correspond to the ionizations evaluated by photoelectron spectroscopy are shown in Figure 8. The elemental characters of the ionizations are listed in Table 2. The highest occupied molecular orbital (HOMO) in **1** and **2** is a primarily symmetric sulfur (S_π^+) out-of-plane orbital. The next highest occupied molecular orbital (HOMO − 1) is a primarily antisymmetric sulfur out-of-plane (S_π^-) orbital. The HOMO shows significant amounts of metal character (with BLYP 19.20% and 15.86% and with SAOP 16.56% and 12.56% for **1** and **2**, respectively). The orbital picture corresponds to the bonding interaction proposed by Lauher and Hoffman.[17] The third highest orbital is primarily a carbon- and

(51) Cacelli, I.; Keogh, D. W.; Poli, R.; Rizzo, A. *J. Phys. Chem. A* **1997**, *101* (50), 9801−9812.
(52) Fourmigué, M.; Lenoir, C.; Coulon, C.; Guyon, F.; Amaudrut, J. *Inorg. Chem.* **1995**, *34*, 4979−4985.

Table 2. Elemental Character (%) of the Valence Orbitals Calculated for **1**−**3**[a]

		$Cp_2Ti(S_2C_2H_2)$ (**1**)		$Cp_2Ti(bdt)$ (**2**)		$Cp_2Ti(pdt)$ (**3**)	
method	atom	BLYP	SAOP	BLYP	SAOP	BLYP	SAOP
HOMO	Ti	19.20	16.28	15.86	12.56	<1	<1
	S	43.80	47.13	43.66	46.31	82.65	83.25
	C_α	19.51	20.01	12.46	12.72	<1	<1
	C_{Cp}	7.52	7.53	8.86	8.77	10.43	9.96
	C_{other}	n/a	n/a	10.24	10.72	2.36	2.49
HOMO − 1	Ti	3.14	2.97	<1	<1	11.28	8.06
	S	68.46	69.42	65.58	66.54	49.35	52.69
	C_α	6.62	6.76	<1	<1	<1	<1
	C_{Cp}	15.71	14.66	10.35	9.95	28.88	26.86
	C_{other}	n/a	n/a	19.83	19.12	<1	<1
HOMO − 2	Ti	12.18	10.76	9.90	8.47	17.81	16.79
	S	12.35	13.21	9.01	9.52	64.34	61.68
	C_α	12.46	11.95	11.61	11.30	1.22	1.24
	C_{Cp}	52.20	52.69	49.16	49.89	6.02	5.58
	C_{other}	n/a	n/a	9.76	9.51	<1	<1

[a] C_α are the C atoms bonded to the S atoms in the M−S−C−C−S metallocycle. C_{Cp} includes all Cp C atoms. C_{other} includes the remaining C atoms.

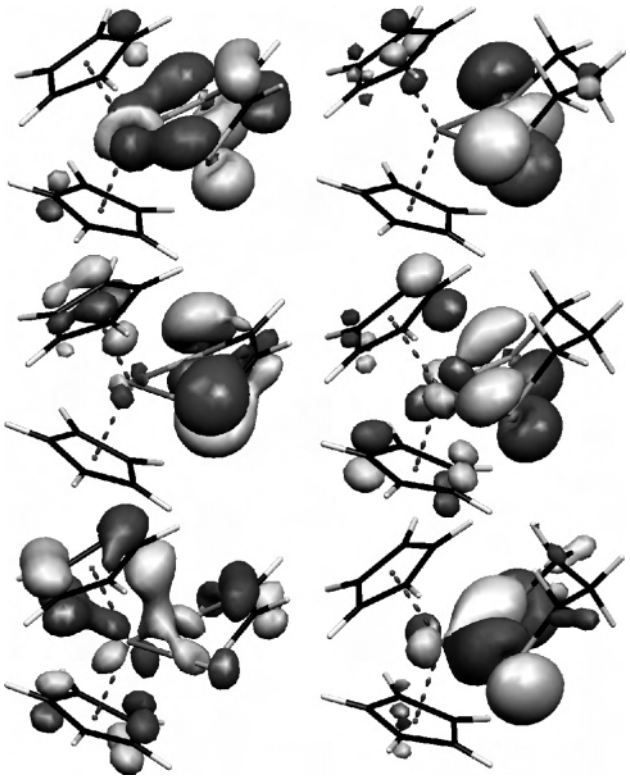

Figure 8. Calculated frontier orbitals (HOMO, HOMO − 1, and HOMO − 2, top, middle, and bottom, respectively) of **1** (left) and **3** (right). All contours have the same cutoff level (0.05).

titanium-based orbital and corresponds to part of the η^5-Cp−Ti bonding orbital manifold. This orbital corresponds to the Cp−Ti orbital described by Reinhold et al.[20] as being raised in energy due to mutual ligand influence from the folding of the dithiolate group.

The separation in energy between the HOMO and HOMO − 1 is different for **1** and **2** (0.70 and 0.22 eV, respectively). This is presumably due to different inductive effects of the ligands and the greater involvement of the benzene ring in the π-system of the ligand for **2**.

Figure 3 shows that the geometry at sulfur for **3** is similar to that for **1** and **2** because the chair conformation adopted by the saturated chelate skeleton of **3** leads to folding along the S−S vector. However, the experimental gas-phase photoelectron spectra (Figure 4) and the DFT calculations (Figure 8) clearly show that the electronic structure of **3** is dramatically different from **1** and **2**. For **3** the HOMO is now the primarily S_π^- orbital, and the HOMO − 1 the primarily S_π^+ orbital (Figure 8). Thus, the order of these orbitals for **3** is reversed compared to those of **1** and **2**. This reversal is ascribed to the effect of the unsaturated chelate skeleton of the dithiolate ligands of **1** and **2**, which effectively couples the pπ orbitals of the two S atoms, thereby raising the level of the S_π^+ to be higher than the level of the S_π^-. To illustrate this point, note that the HOMO of **1** shown in Figure 8 indicates a strongly antibonding interaction between the S 3p orbitals and the C−C π orbital of the enedithiolate. The strong coupling of the S p_π orbitals by the unsaturated linkage observed in **1** and **2** is not apparent in **3**, even though the chair conformation of the saturated dithiolate ligand produces a similar fold along the sulfur−sulfur vector of **3**. The S_π^+ orbital (HOMO − 1) of **3** shows some metal character (with BLYP 11.28% and with SAOP 8.06%), but this is less than for **1** and **2** (see above), presumably because the conformation induced folding allows for some mixing. The first and second bands of **3** differ in energy by 0.61 eV; this energy difference is similar to that shown in 1,3-dithiane (0.41 eV) for the bands assigned to S_π^- and S_π^+.[53,54] This difference is assigned as being due to a through-space interaction;[53] the S−S distance in 2-phenyl-1,3-dithiane is 3.037,[55] whereas that in **3** is 3.335 Å. The third orbital in **3** is a pseudo-σ Ti−S type orbital and not a Cp-based orbital as described for **1** and **2**, consistent with there being no mutual ligand influence in this case and the Cp−Ti-based orbitals being in the same energy range as for Cp_2TiCl_2.[48]

Calculations of the transition energies corresponding to the electronic absorption excitations were carried out using both time-dependent density-functional theory (TDDFT) and the Slater transition state formalism (see Table 3). The first two transitions in all cases are from S_π orbitals to the LUMO,

(53) Vondrák, T.; Bastl, Z. *J. Mol. Struct.* **1987**, *160*, 117−126.
(54) Sweigart, D. A.; Turner, D. W. *J. Am. Chem. Soc.* **1971**, *94* (16), 5599−5603.
(55) Kalff, H. T.; Romers, C. *Acta Crystallogr.* **1966**, *20*, 490−496.

Table 3. Experimental and Calculated Transition Energies (cm^{-1}) for the Low-Energy Electronic Absorptions of **1**−**3** (with Oscillator Strength ×100 in Parentheses)

	1st excitatn	2nd excitatn	3rd excitatn
		$Cp_2Ti(S_2C_2H_2)$, **1**	
obsd	15 500	19 300	23 700
BLYP Slater	11 606	17 083	21 245
assgnt	HOMO → LUMO	HOMO − 1 → LUMO	HOMO → LUMO + 1
TD BLYP	15 977 (1.74)	19 232 (0.64)	21 112 (0.42)
assgnt	HOMO → LUMO	HOMO − 1 → LUMO	HOMO → LUMO + 1
TD SAOP	16 962 (2.00)	20 610 (0.67)	22 410 (0.03)
assgnt	HOMO → LUMO	HOMO − 1 → LUMO	HOMO → LUMO + 2
		$Cp_2Ti(bdt)$, **2**	
obsd	16 400		22 400
BLYP Slater	11 840	13 405	20 059
assgnt	HOMO → LUMO	HOMO − 1 → LUMO	HOMO − 2 → LUMO
TD BLYP	14 924 (0.59)	15 357 (2.95)	20 929 (0.48)
assgnt	HOMO − 1 → LUMO	HOMO → LUMO	HOMO − 2 → LUMO
TD SAOP	16 517 (3.22)	16 580 (0.52)	22 912 (0.55)
assgnt	HOMO → LUMO	HOMO − 1 → LUMO	HOMO − 2 → LUMO
		$Cp_2Ti(pdt)$, **3**	
obsd	18 600		27 800
BLYP Slater	13 219	17 397	21 389
assgnt	HOMO → LUMO	HOMO − 1 → LUMO	HOMO − 2 → LUMO
TD BLYP	14 835 (1.04)	19 515 (0.16)	20 073 (0.86)
assgnt	HOMO → LUMO	HOMO − 1 → LUMO	HOMO − 1 → LUMO + 1
TD SAOP	17 210 (1.17)	21 632 (0.22)	22 604 (0.72)
assgnt	HOMO → LUMO	HOMO − 1 → LUMO	HOMO − 1 → LUMO + 1

i.e., LMCT bands. Description of the bands in the region from 22 000 to 36 000 cm^{-1} is complicated by the presence of multiple transitions. However, the S_π to LUMO bands are sufficiently distinct for some discussion. The estimations by the Slater method are lower in energy than the estimates by both TDDFT methods for all S_π to LUMO transitions.

The estimations by TDDFT methods correspond closely to the bands observed in the electronic absorption spectra of **1** and **2**. In the spectrum of **1** there is some separation between the first and second bands (>3000 cm^{-1}). The first band (at 15 500 cm^{-1}) is predicted to be S_π^+(HOMO) → LUMO, and the second (at 19 300 cm^{-1}), S_π^-(HOMO − 1) → LUMO. In the spectrum of **2** the band at 16 400 cm^{-1} is predicted to contain contributions from both the S_π^+ → LUMO, and the second, S_π^- → LUMO. The combined area of the first two bands in the normalized spectrum of **1** is approximately the same as the area of the first band of **2**, consistent with this prediction.

The first band of the spectrum of **3** is at a higher energy than the first bands of **1** or **2** and at higher energy than the first band predicted by Slater or TD methods. The predicted first band (at 18 600 cm^{-1}) is S_π^- → LUMO in this case due to the change in ordering of the orbitals (Figure 6). It has an energy and normalized area similar to those of the S_π^- → LUMO observed for **1** (at 19 300 cm^{-1}). The S_π^+ → LUMO is predicted to be of low intensity and is either absent or part of the bands starting at 27 800 cm^{-1}.

The S_π^+ → LUMO is significantly more intense for **1** and **2** than it is for **3**. The S_π^- → LUMO is evident in **1**−**3**, but for **1** and **2** it is not as intense as the S_π^+ → LUMO. This may be an indication of the importance of the unsaturated ligand for increasing the availability of charge transfer between the ligand and the metal center. This is presumably due to the increased overlap of metal- and sulfur-based orbitals.

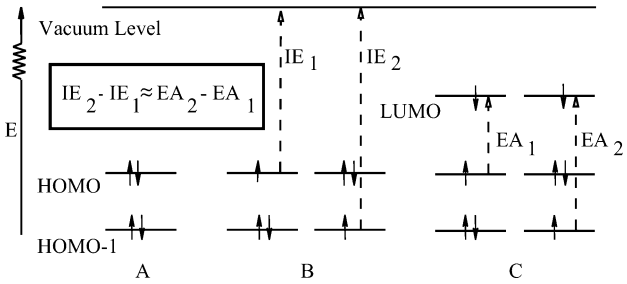

Figure 9. Comparison of transitions that occur from the ground state (A) to the first and second excited states in photoelectron spectroscopy (B) and electronic absorption (C).

Figure 9 summarizes the energy relationships of the HOMO (S_π^+) and HOMO − 1 (S_π^-) levels for **1** and **2** in the ground state and in the photoelectron (PES) and electronic absorption (EA) experiments. A complication in such comparisons is that the excited states produced are different for the PES and EA experiments. The PES experiment produces a cation in which one electron has been lost from an occupied orbital. The EA experiment produces a neutral species with an electron in the LUMO and a singly occupied HOMO, HOMO − 1, etc. The final states for the PES and EA processes have different reorganization energies and different configurational interactions. Nonetheless, information from PES and EA spectroscopies have been compared previously. For example, combined PES and EA data have been used in the interpretation of the optical properties of coumarins[56,57] and in the study of the electronic structure of the oxomolybdenum bis(dithiolate) ions, $[MoO(S_2C_2(CN)_2)_2]^{n-}$.[58] For **1** the PES bands corresponding to S_π^+ and S_π^- are

(56) Novak, I.; Kovac, B. *J. Electron Spectrosc. Relat. Phenom.* **2000**, *113* (1), 9−13.
(57) Kovac, B.; Novak, I. *Spectrochim. Acta, A* **2002**, *58A* (7), 1483−1488.
(58) Waters, T.; Wang, X. B.; Yang, X.; Zhang, L.; O'Hair, R. A.; Wang, L. S.; Wedd, A. G. *J. Am. Chem. Soc.* **2004**, *126* (16), 5119−5129.

separated by 0.70 eV (5600 cm^{-1}), and the electronic absorption bands corresponding to transitions from S_π^+ and S_π^- to the LUMO are separated by 0.47 eV (3800 cm^{-1}). For **2** the PES bands corresponding to S_π^+ and S_π^- are within 0.22 eV (1800 cm^{-1}), and the electronic absorption bands corresponding to transitions from S_π^+ and S_π^- to the LUMO are indistinguishable (within 1000 cm^{-1}).

Conclusion

The relationship between the fold angle of dithiolene ligands and the occupancy of the metal-based "in plane" orbital has been established in metallocenes[16,17] and pyrazolylborate compounds.[26,27] This work further confirms this relationship. Comparison of the benzenedithiolate and ethenedithiolate system shows that folding is dependent upon the presence of an unsaturated carbon−carbon bond (ene group) linking the two S atoms and is not an effect of crystal packing. However, the nature of the substituent of the ene group does have an effect on the detailed electronics of the system. The differences in energy between the first and second ionizations, the degree of folding, and relative amounts of metal and sulfur character in the HOMO are dependent upon the nature of the substituents.

To observe the "dithiolate-folding effect" there must be coupling between the S p_π orbitals and the C p_π orbitals derived from the M−S−C−C−S ligand backbone. Such coupling raises the energy of the S_π^+ orbital above that of the S_π^- orbital and poises the energy of the S_π^+ orbital for interaction with the metal-based "in plane" orbital. This electronic structure facilitates the "dithiolate-folding effect" as only the S_π^+ has the correct symmetry to overlap with metal-based "in plane" orbital. In a saturated dithiolate ligand, as shown in this work, the coupling between the pπ orbitals on the two S atoms is greatly reduced and the ordering of the S_π orbitals is reversed in comparison to the unsaturated dithiolate. Thus, although ligand design can control the relative conformations of the two Sπ orbitals of a coordinated dithiolate to orient the S p_π orbitals toward the metal acceptor orbital (as in **3**), effective electronic coupling of these orbitals requires an unsaturated linkage (as in **1** and **2**).

The active sites of mononuclear molybdenum-containing enzymes contain at least one pyranopterin ligand that forms a five-membered ring containing molybdenum and an enedithiolate. Each part of the ring appears to be essential for the functioning of the enzyme. Molybdenum d^0 and d^2 states can be stabilized or destabilized by control of the folding via hydrogen-bonding interactions between the protein backbone and the molybdenum−pyranopterin units. The sulfur π-orbitals allow strong mixing of metal- and ligand-based character in the HOMO, permitting efficient electron transfer and control of the chemical potential. The enedithiolate unit raises the energy of the sulfur-based π-orbitals for optimal overlap and electron transfer. Mutual ligand influence between the enedithiolate of the pyranopterin and other ligand valence orbitals may also be present in the enzyme center and modulate the chemistry of the molybdenum center.

Acknowledgment. We gratefully acknowledge support of this research by the National Institutes of Health (Grant GM-37773 to J.H.E.) and the National Science Foundation for funds for the mass spectrometer (Grant CHE-9601809). We thank Dr. A. Somogyi for mass spectrometry. We thank Prof. D. L. Lichtenberger for helpful discussions. We thank the reviewers for helpful comments.

Supporting Information Available: Computationally derived geometry-optimized coordinates and selected eigenvalues of orbitals of **1**−**3**. This material is available free of charge via the Internet at http://pubs.acs.org.

IC049207+